Vibrational imaging of tablets by epi-detected stimulated Raman scattering microscopy

Supplementary Information

Mikhail N. Slipchenko,[a] Hongtao Chen,[b] David R. Ely,[c] Yookyung Jung,[d] M. Teresa Carvajal,*[c] Ji-Xin Cheng*[ab]

[a]*Weldon School of Biomedical Engineering, Purdue University, West Lafayette, IN, 47907, USA.*

[b]*Department of Chemistry, Purdue University, West Lafayette, IN, 47907, USA.*

[c]*Department of Industrial and Physical Pharmacy, Purdue University, West Lafayette, IN, 47907, USA.*

[d]*Department of Physics, Purdue University, West Lafayette, IN, 47907, USA.*

[*]To whom correspondence should be addressed. Tel: 765-494-4335. Fax: 765-494-1193. E-mail: jcheng@purdue.edu; Tel: 765 496-6438. Fax: (765) 494-6545. E-mail: arvajal@pnhs.purdue.edu

Figure S1. Digital image of tablets from Pfizer (Norvasc), Apotex, Greenstone, Ethex, Teva Pharmaceutical, and Upsher-Smith Laboratories, respectively.

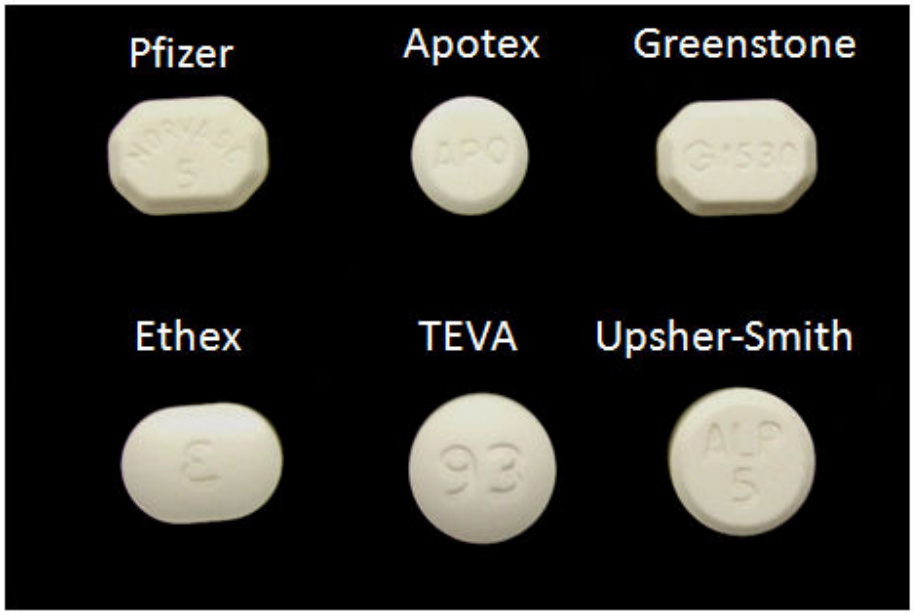

Figure S2. AFM imaging of a tablet (Pfizer). (A) Small area AFM image. Scale bar is 5 μm. (B) Long line scans performed at different areas on the surface.

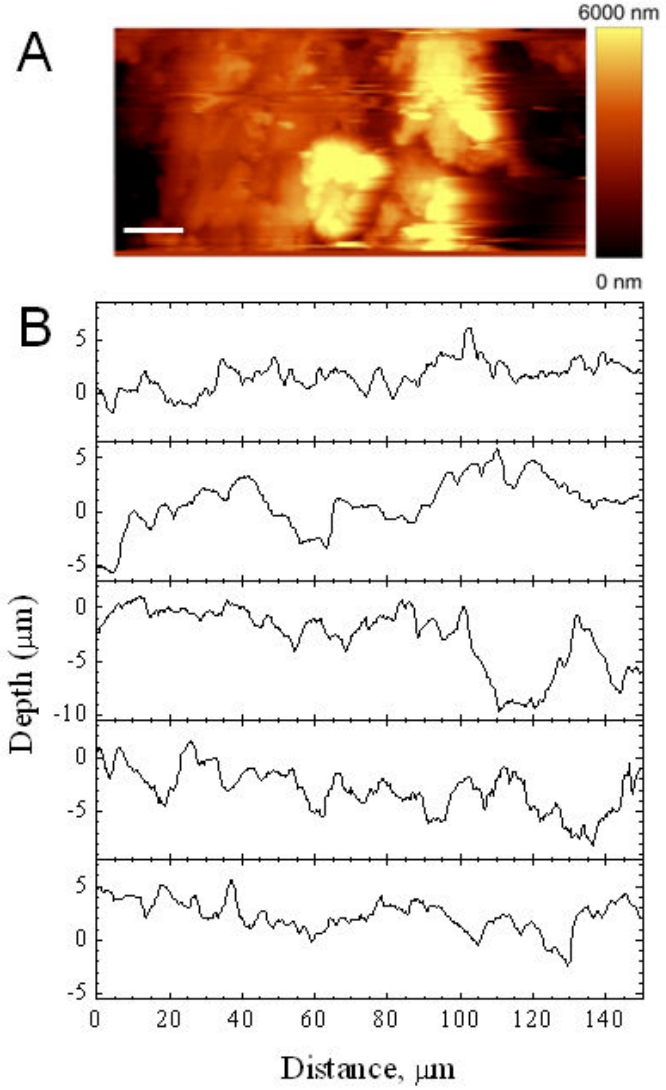

SRS depth profiles

In order to estimate SRS imaging depth of field for 10× (0.40 N.A.) and 20× (0.75 N.A.) objectives we performed SRS depth scan through glass/oleic oil interface with step size of 1 μm. The ω_p-ω_S difference was set to 2850 cm^{-1} to be in resonance with CH_2 symmetric stretch of oil. The depth profiles are shown in Fig. S3A. These profiles represent integrated SRS intensity as objective focal volume passes through glass/oil interface. Therefore, the first derivative of such depth profile will return the SRS focal volume axial profile. The derivatives of two depth profiles are shown in Fig. S3B together with Lorentzian fit. The fit gives full width at half maximum (FWHM) of 7 μm for 20× objective and 24 μm for 10× objective. Because depth of field has a quadratic dependence on numerical aperture (N.A.) the 3.4 times increase in depth of field of 10× (0.40 N.A.) objective vs. 20× (0.75 N.A.) is expected.

Figure S3. SRS depth of field for 10× and 20× objectives. (A) SRS intensity axial profile through glass/oil interface for 10× (black circles) and 20× (red squares) objectives. (B) The first derivatives of profiles in A. The dashed lines are Lorentzian fir of derivatives.

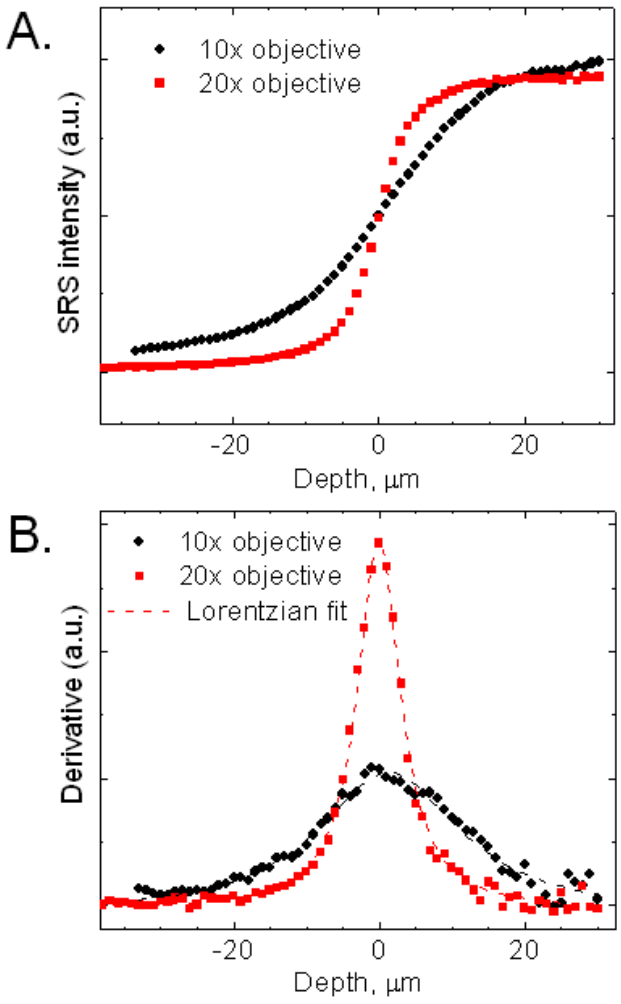

Compound Raman analysis of tablet (Pfizer).

The validity of SRS image shown in Fig. 2C was confirmed by confocal Raman analysis performed at the points of interest (see Fig. S4). Note, that sample was analyzed at the SRS microscope using Raman microspectroscopy capabilities of the setup (see Fig. 1). In Fig. S4, the Raman spectra at position 1 to 5 which correspond to positions of MCC, DCPA, AB, SSG and MS particles are similar to those of pure components in Fig. 2A. Due to the large depth of field the confocal Raman spectra show some contribution of Raman peaks from different components. For example, the spectrum 5 in Fig. S3B is very similar to spectrum of MS shown in Fig. 2A but has a contribution from spectrum of AB as indicated by asterix.

Figure S4. Raman spectral analysis of the SRS image. (A) SRS image from Fig. 2C with indicated positions where 5 Raman spectra were obtained. (B) Raman spectra obtained at positions indicated in (A). Excitation wavelength is 707 nm, 6 mW power at the sample. 20× air objective (Olympus, N.A. = 0.75) was used. Scale bar is 100 µm.

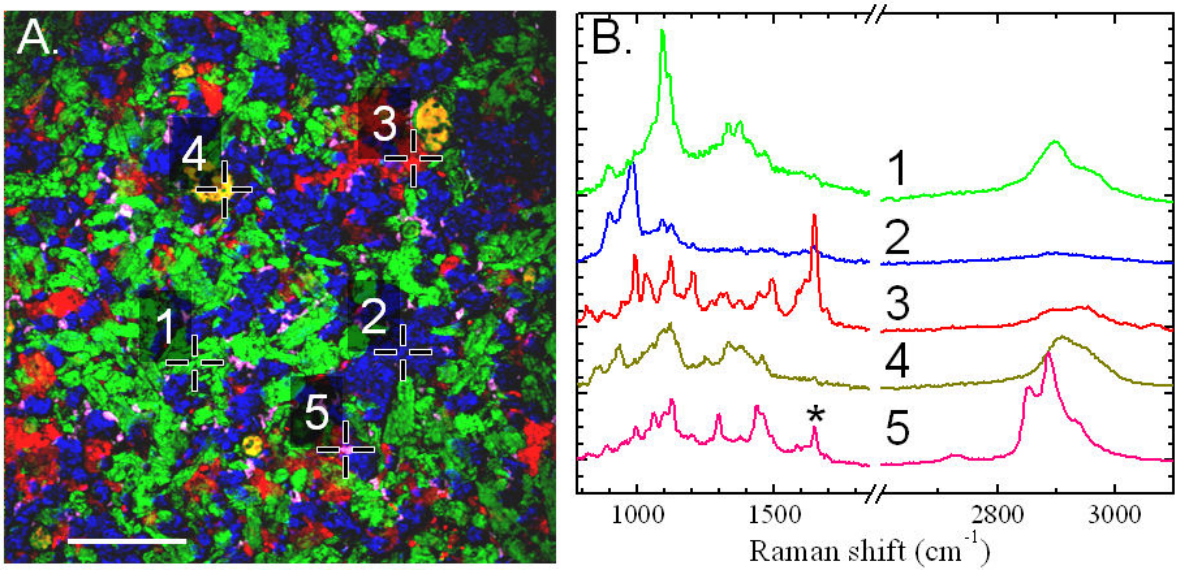

Figure S5. High resolution SRS image. (A) SRS image of AB at 1650 cm^{-1}. (B) Intensity profile alone the dashed line in (A). 60× water-immersion objective was used (Olympus, N.A. = 1.2).

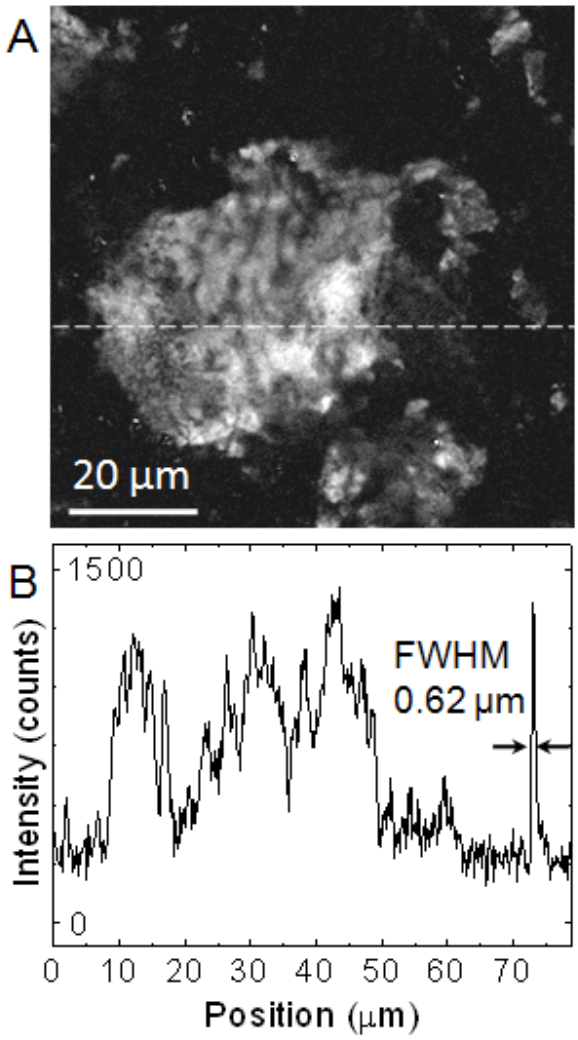

Linear Scale of Segregation Analysis.

We modeled a tablet as a binary mixture of non-diffusive components A and B, where A is a drug component and B accounts for the rest of the components. Since there is no diffusion, the concentration of A, denoted as *a*, can be either 1 or 0 for any given pixel in the image. Assuming that segregated regions, i.e, drug particles or agglomerates, are spherical, the average diameter of the segregated regions is given by the linear scale of segregation , *S*, which is defined as:[1, 2]

$$S = \int_0^\infty R(r)dr \tag{1}$$

where *R(r)* is the correlation function between the concentrations of component *A* at points separated by a distance *r*:

$$R(r) = \overline{(a_1 - \overline{a})(a_2 - \overline{a})} \Big/ \overline{(a - \overline{a})^2} \tag{2}$$

Here a_1 and a_2 are concentrations of A at two points separated by distance *r*. $\overline{(a-\overline{a})^2}$ is mean square deviation of all the concentrations from the mean $\overline{a}$. Due to the long computational time required to compute *R(r)* from all pixels in a 512×512 pixel image, we randomly selected 20,000 pixels from within the first 412 pixel rows and 412 pixel columns of a binarized image. For each of these pixels, we used 100 pixels to the right and 100 pixels down to generate the correlation function. The threshold for image binarization was chosen such that noise in the resulting black and white image was minimized.

Statistical Analysis. Student's *t*-Test and analysis of variance (ANOVA) between groups were performed to estimate the statistical differences between the linear scales of segregation in different samples at the 5% significance level.

Quantitative Analysis of Drug Distribution within Tablets from Six Manufacturers.

To demonstrate the capability of SRS for high-speed screening of tablets, we mapped the distribution of AB in tablets made by six different companies (Fig. S1). For quantitative analysis, we used a 20× air objective (N.A.=0.75) for SRS imaging of large areas. To quantify the drug distribution uniformity, multiple images of different areas within each tablet were acquired (see Fig. S6) for correlation analysis. The correlograms and calculated linear scales of segregation are shown in Fig. S7. The correlograms of all samples are positive which indicates the absence of long range order in drug spatial distribution. Assuming that the segregated regions are primary particles, the calculated linear scales of segregation indicate that tablets from Pfizer, Greenstone and Teva Pharmaceutical have a similar AB mean particle size of about 7 μm (p = 0.48). Note, that above estimates are based on surface exposure of the particles and may differ for particle in the volume. The tablet from Apotex is similar to the tablet from Upsher-Smith Laboratories with AB mean particle size of about 11 μm (p = 0.25). The AB mean particle size in the tablet from Apotex is different from that in tablets from Pfizer, Greenstone and Teva Pharmaceutical (p = 0.0042) whereas AB mean particle size in the tablet from Upsher-Smith Laboratories is not (p = 0.22). Finally, the tablet from Ethex has the largest AB mean particle size of 17 μm and is statistically different from the AB mean particle size in other five tablets (p<0.0001).

Figure S6. Distribution of AB in tablets from six manufacturers. A, B, C, D, E, and F correspond to images of tablets from Pfizer (Norvasc), Apotex, Greenstone, Ethex, Teva Pharmaceutical, and Upsher-Smith Laboratories, respectively. AB is imaged at 1650 cm^{-1} Raman shift. Four randomly chosen areas are imaged for each sample. 20× air objective (Olympus, N.A. = 0.75) was used.

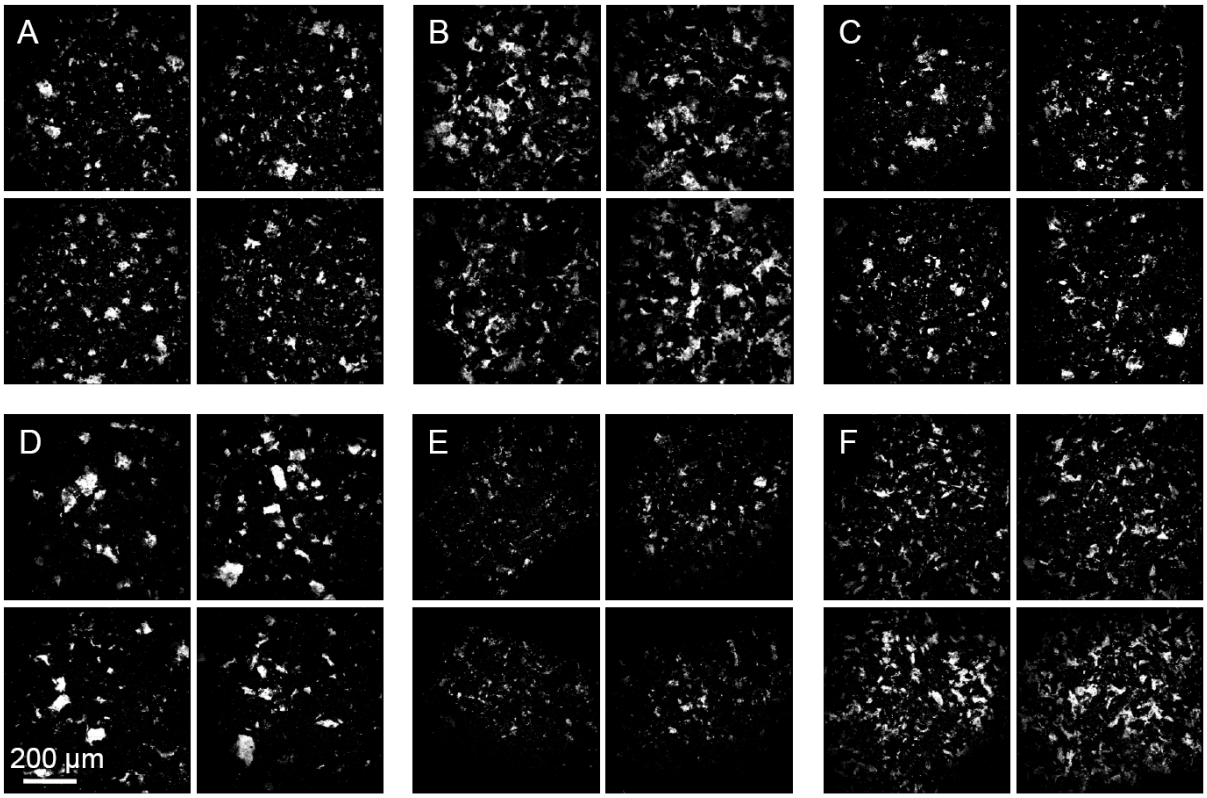

Figure S7. Correlograms and linear scale of segregation calculated from distribution of AB in tablets from six manufacturers. (A) The correlograms. (B) Linear scale of segregation. The error bars are the standard deviation (n=4) of the linear scales of segregation. The correlograms and linear scale of segregation were calculated from four images per sample.

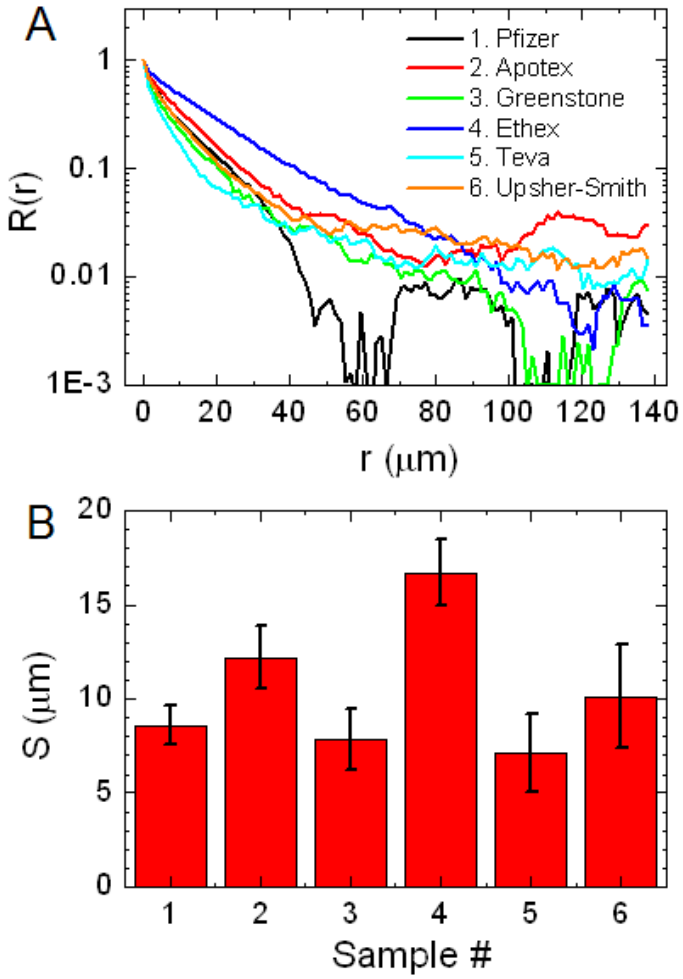

References.

1. P. V. Danckwerts, *Appl. Sci. Research*, 1952, **3**, 279-296.
2. A. Kukukova, J. Aubin and S. M. Kresta, *Chem. Eng. Res. Des.*, 2009, **87**, 633-647.